Wireless ATM-Based Multicode CDMA Transport Architecture for MPEG-2 Video Transmission

PO-RONG CHANG, MEMBER, IEEE, AND CHIN-FENG LIN

Invited Paper

In this paper, we present a generic ATM-based multicode code division multiple access (CDMA) transport architecture for the Motion Picture Experts Group phase 2 (MPEG-2) compressed video services over a bandlimited mobile channel with the emphasis of wireless asynchronous transfer mode (ATM) cell design, spreading code management, and the impact of CDMA systems on the video services. Such services allow users to share novel MPEG-2 video applications without any geographical restrictions. The ATM technique is especially well suited for variable bit rate (VBR) MPEG-2 video because of its ability to allocate bandwidth on demand to these services. However, since the mobile radio has a limited channel capacity, the overall capacity of the traditional ATM-based CDMA system may not be sufficient to accommodate the MPEG-2 video services requested by the multiple mobile users simultaneously. To tackle this difficulty, a multicode CDMA technique is proposed to provide multiple VBR MPEG-2 video services by varying the number of spreading codes assigned to each MPEG-2 video in order to meet its dynamic throughput requirement. Moreover, both the multipath fading and interference on CDMA radio channels tend to cause significant transmission error and MPEG-2 bit streams are very vulnerable to these errors. Powerful forward error correction (FEC) codes are therefore necessary to protect the video data so that it can be successfully transmitted at acceptable signal power levels. Two separate FEC code schemes are applied to the header and payload of an ATM cell containing MPEG-2 video data, respectively. The ATM cell header is protected by a relatively powerful FEC code to ensure the low average cell loss rate (CLR). On the other hand, the ATM cell payload is encoded for varying degrees of error protection according to both the priority and statistical behavior of the payload data in MPEG-2 videos. An adaptive FEC code combining scheme is proposed to provide the good protection for payload data with the maximization of its code rate in order to minimize the extra bandwidth for FEC overhead. Two typical MPEG-2 test sequences are conducted to evaluate the effectiveness of our system.

Keywords*—*MPEG video, multicode code division multiple access (CDMA), wireless ATM.

Manuscript received January 1, 1998; revised March 25, 1998. This work was supported in part by the National Science Council, Taiwan, R.O.C., under Contract NSC 88-2213-E-009-128.

The authors are with the Department of Communication Engineering, National Chiao-Tung University, Hsin-Chu, Taiwan.

Publisher Item Identifier S 0018-9219(99)07477-0.

I. INTRODUCTION

Future third-generation mobile communication [1]–[3] based on the asynchronous transfer mode (ATM) principle is designed to support a wide variety of multimedia services with diverse statistical characteristics and quality of service (QoS) requirements at cell and call levels. Among the various kinds of services, video service is becoming an important component of multimedia communications. A number of video coding schemes have been proposed for the compression of video signals that generate a high bit-rate stream via the ATM broad-band networks. A well-known coding scheme called the Motion Picture Expert Group (MPEG) is emerging as a major international standard for multimedia applications [4]. The MPEG specification was developed specifically to allow the transmission of VCR-quality digital images at a data rate of approximately 1–1.5 Mbits/s. IS01172 is also sometimes referred to as MPEG-1. Another specification known as MPEG-2 has been developed to support higher resolution images. The MPEG video compression algorithm relies on two basic techniques: block-based motion compensation for reduction in temporal redundancy and discrete cosine transform (DCT) for reduction in spatial redundancy. MPEG is able to reduce the raw image data by twenty to fiftyfold. Because of the conflicting requirements of random access and highly efficient compression, three main picture types are defined. Intrapictures (I pictures) are coded without reference to other pictures and points for random access. Predictive (P) pictures are coded with reference to previous I- or P-frames. Bidirectionally predictive (B) pictures are coded with reference to a previous I- or P-frame as well as the future I- or P-frame. As a result, the MPEG encoder produces a variable bit-rate (VBR) compressed video bit stream in which instantaneous bit rates vary widely with scene content. Moreover, the correlation between consecutive pictures is very low since MPEG video generates very bursty traffic that changes dynamically on a picture-by-picture basis depending on

coding mode. The most interesting standard currently under development is MPEG-4, which offers universal access capabilities in error-prone environments and content-based scalability. Before the MPEG-4 standard has been completed, this paper is aimed at investigating the wireless transmission of the defined benchmark MPEG-2 videos. It is expected to provide the design philosophy of a generic wireless transport architecture for the forthcoming MPEG-4 as well as the other widely used benchmark video codecs, i.e., H.261 and H.263 families.

The ATM technology utilizes the nature of the traffic to allocate effectively the network resources via statistical multiplexing. According to the traffic categories as defined in the ATM Forum TM4.0 (ATM service categories), the first class includes all the jitter-tolerant applications [unspecified bit rate (UBR) and available bit rate (ABR) service categories], while the second includes all the real-time applications [constant bit rate (CBR) and VBR service categories]. This paper focuses on the development of the code division multiple access (CDMA) transport architecture for the VBR video service as well as CBR video service. Wireless ATM has become an important research topic over the last three years [5]–[7]. Such services allow users to share novel multimedia applications without any geographical restrictions. Zhang *et al.* [8] have investigated an application of wireless ATM techniques to the transmission of MPEG video. However, they did not consider the problem of transmitting multiple high VBR MPEG videos over a narrow-band wireless channel simultaneously. This problem could be ameliorated via multicode CDMA transmission [9]–[11]. In other words, high data transmission rates are achieved by allocating more than one spreading code to a single MPEG video in order to create more than one virtual channel for the MPEG video. As VBR MPEG video traffic is both delay sensitive and has a high degree of burstiness, it is commonly believed that a large number of spreading codes corresponding to the peak source bit rate must be reserved for the video transmission to satisfy its QoS requirements. The reservation of a large number of spreading codes assigned to each MPEG video seems extremely inefficient for the transmission of multiple MPEG videos over a narrow-band radio channel. Taking into consideration that the ratio between the peak and average bit rate for VBR MPEG video is generally high, this implies that a large portion of spreading codes remains unused when the low bit-rate B-frames are transmitted via the multicode CDMA network. To increase the efficiency in the spreading code assignment mechanism, we designed an algorithm which dynamically allocates an appropriate number of codes to each MPEG video on the basis of its actual source rate. Furthermore, in order to avoid the self-interference that a MPEG employing multiple codes may incur, the multiple codes to/from one MPEG should be made orthogonal. This particular spreading coding scheme is called the concatenated orthogonal/pseudonoise (PN) spreading code [10] which is capable of subdividing a high bit-rate MPEG stream into several parallel lower basic bit-rate streams without self-interference. In addition, the quality of received MPEG video may degrade severely when the ATM cell loss occurs due to the multipath fading, interference, and channel noise. In Section III, an adaptive forward error correction (FEC) code combining scheme has been proposed to eliminate the cell loss according to both the statistical behavior and the importance of data types in MPEG video. The objective of code combining is to maximize its code rate and to provide good error protection with reasonable time delay. Simulation results show that this FEC code combining scheme is able to protect the MPEG video data and achieve the good received picture quality without a large amount of extra FEC overhead data. Moreover, Zhang and Lee [12] have shown that the error concealment techniques are very effective in improving both objective and subjective quality of received MPEG video via multipath fading channels. Therefore, in Section VII, a modification of both the spatial and temporal error concealment techniques [13]–[18] is applied to recover the received MPEG video with information loss. Finally, a number of typical MPEG video test sequences are conducted to verify the effectiveness of the proposed ATM-based multicode CDMA system in various aspects.

II. Overview of MPEG Standard

The MPEG video international standard [4] specifies the coded representation of the video data. The video source coding is based on motion compensated hybrid DCT coding which employs two basic techniques: motion compensation for the reduction of temporal redundancy and DCT transform compression for the reduction of spatial redundancy. In order to achieve the highly efficient compression and meet the conflicting requirements of random access, the input video is divided into units of group-of-pictures (GOP's) consisting of an intra (I) picture, coded without reference to other pictures, and arrangement of predictive (P) pictures, coded with reference to previous (I or P) picture, and bidirectionally predictive (B) pictures, coded with reference to an immediate previous (I or P) picture, as well as an immediate future (P or I) picture. The I picture frame at the beginning of a GOP serves as a basic entry point to facilitate random seek or channel switching and also provides coding robustness to transmission error, but it is coded with only moderate compression to reduce the spatial redundancies. P picture frames are coded more efficiently using motion compensated prediction from a past I or P picture frame and are generally used as a reference for further prediction. B picture frames provide the highest degree of compression, but require both past and future reference pictures for motion compensation. It should be mentioned that B pictures are never used as references for prediction. A GOP is defined by its length N_{GOP}, which is the distance between I pictures. An example of a GOP in MPEG is presented in Fig. 1, where I, P, and B denote picture encoding in the intrapicture mode, predicted mode, and bidirectionally predicted mode, respectively. The GOP sequence of Fig. 1 with $N_{\mathrm{GOP}} = 6$ is, IBBPBBI.

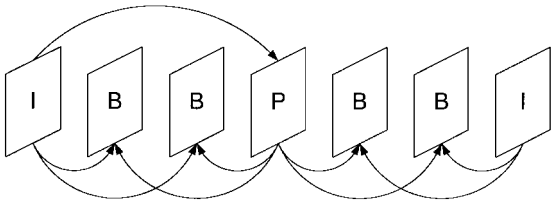

Fig. 1. Example of MPEG GOP.

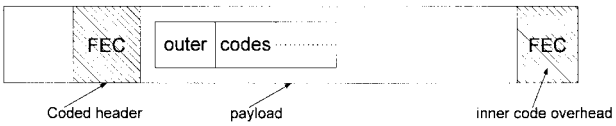

Fig. 2. Logical structure of a wireless ATM cell with outer/inner FEC code combining.

The macroblocks of 16 × 16 pixels are the basic coding units for the MPEG algorithm. Each macroblock is divided into four blocks, where each block contains 8 × 8 pixels. The main extension from monochrome video to color is the addition of two 8 × 8 chrominace blocks to the macroblock. A row of macroblocks that makes up a horizontal strip in the image is called a slice and a number of slices are combined to form a picture. The coding mode of each macroblock within a specific picture depends on its picture type. For I pictures, a DCT is performed on each block. The resulting two-dimensional block of DCT coefficients is quantized and scanned in a zig-zag order to convert it into a one-dimensional string of quantized DCT coefficients. Run-length coding is used for the quantized coefficient data. The predicted pictures (P and B) use motion compensated prediction of the contents of the macroblock based on past or future reference pictures. This prediction is subtracted from the actual data in the current macroblock to form an error signal. The prediction error is coded like the intracoded macroblocks.

III. Design of Wireless ATM Cells for MPEG Videos

Zhang *et al.* [8] have proposed a wireless ATM cell model for MPEG-2 videos which is quite similar to Lei's cell structure [19] with a header of 5 bytes and a payload of 48 bytes for MPEG-2 over wireline ATM networks. However, wireless multipath fading, interference, and noise tend to cause significant ATM cell loss. A single cell loss will result in the severe MPEG image quality degradaion when the cell carries a large amount of payload data. Lin and ElZarki [24] have suggested that the wireless ATM cell should not carry too much data to avoid the loss of large amount of image data in a single cell loss. Furthermore, FEC codes are necessary to protect either ATM cell header or payload data so that it can be successfully transmitted at an acceptable signal power level in order to provide adequate image quality. However, the extra bandwidth for FEC overhead for wireless ATM cells seems critical in the narrow-band wireless networks. This section will investigate the appropriate tradeoff between error control and MPEG video transmission quality.

Table 1
Priority Rank for the Different Data Types Within Each Frame (I, P, B)

I-frames	1. Frame header
	2. Slice headers
	3. Macroblock headers
	4. DC coefficients
	5. Low frequency AC coefficients
	6. High frequency AC coefficients
P- and B-frames	1. Frame header
	2. Slice headers
	3. Macroblock headers
	4. Motion vectors
	5. DC coefficients
	6. Low frequency AC coefficients
	7. High frequency AC coefficients

Two separate error control coding schemes are applied to the header and payload of a wireless ATM cell illustrated in Fig. 2. Usually, an ATM cell consists of a 5-byte header. Raychaudhur [3] showed that the ATM header over a wireless network could be compressed to either 2 or 3 bytes. For simplicity, a 2-byte compressed header will be used in the wireless ATM cell. A shortened Bose–Chaudhuri–Hocquenghem (BCH) code of (31,16) is suggested to protect this header. On the other hand, a concatenated error control coding scheme with unequal error protection (UEP) is applied to the payload in accordance with two priority categories, i.e., the priority for each picture frame in the temporal domain and the importance of data types belonging to the frame. There are three priority levels involved in three frame types belonging to the MPEG video at three different time points in the temporal line (domain). For the MPEG bit stream, I-frame (I picture frame) information tends to be the most important data for transmission because the effect of losses on this frame will tend to propagate, until the next I-frame, and then causes no temporal prediction for P- and B-frames. The P- and B-frames are, respectively, the medium and the least important data for transmission since P-frame is usually treated as a reference for the temporal prediction of B-frames. Therefore, there are BCH codes with three different error protection levels, i.e., of (255 215), (255 223), and (255, 231) which are used to protect I-, P-, and B-frames, respectively. These codes are called the "inner" FEC codes according to the definition of a concatenated code composed of convolutional and Reed–Solomon (RS) codes [20]. The outer FEC codes are proposed to protect the high-priority data belonging to each frame twice. By analyzing the data types in each of I-, P-, and B-frames, it is found that there are six priority levels for the data in I-frames and seven priority levels for the data in either P- or B-frame shown in Table 1. For example, for I-frames, the highest priority is given to frame header and the lowest priority is given

to high frequency AC coefficients. The frame header is usually included in a resource management (RM) cell with a high error protection which is used to provide the current frame information and its resource management status for mobile receivers before transmitting the ATM cells. Hence, the outer FEC codes are proposed to protect the second, third, and fourth highest priority data [Slice header, macroblock (MB) header, and DC values] in an I-frame, and to protect the second, third, fourth, and fifth highest priority data (Slice header, MB header, motion vectors, and DC values) in both P- and B-frames. Neverthless, the remaining low priority data (AC values) are still protected by the inner codes. For the sake of reducing the implementation complexity, a class of shortened BCH codes is chosen for the design of the outer FEC coding. The next section will discuss more details of the code selection principle for outer codes.

A. Code Selection Principle for Outer Codes According to Data Partitioning

The work by Parthasarthy *et al.* [21], which describes a code selection strategy in the case of a normal RS code scheme for video traffic over wireline ATM networks, is closest to that in this paper. However, in [21], the MPEG video protected by the use of concatenated code according to its priority have not been considered. The objective of code selection is to minimize the outer code overhead and to provide good protection with reasonable time delay. In other words, we choose an appropriate class of outer codes which maximizes the average code rate for a coded ATM cell given by

$$\overline{R}_c = \frac{n_m^c}{(n_h^c + n_p^c)} \tag{1}$$

where n_m^c denotes the average number of message bit in a coded ATM cell, and n_h^c and n_p^c represent the average numbers of bits in a coded header and bits in a coded payload with inner/outer coding, respectively. The maximization of $\overline{R}_c$ is over all the shortened BCH outer codes. Unfortunately, it is hard to characterize $\overline{R}_c$ directly according to the VBR characteristics of the high-priority data in each frame of MPEG video. To overcome this difficulty, the expression of (1) can be approximated by a form in the slice manner

$$\overline{R}_c \approx \frac{\overline{\text{Slice}}}{\overline{\text{CSlice}} + \overline{\text{Code}}_{\text{in}} + \overline{\text{CATMh}}} \tag{2}$$

where $\overline{\text{Slice}}$ is the average number of message bits in a slice, $\overline{\text{CSlice}}$ denotes the average number of bits in a coded slice using outer coding scheme only. $\overline{\text{Code}}_{\text{in}}$ and $\overline{\text{CATMh}}$ represent the average numbers of bits in the inner code overheads and bits in the coded ATM headers for a slice, respectively. Let m denote the number of message bits in the inner code. In other words, each ATM cell with inner coding can carry m message bits per cell. It should be noted that the coded bits generated by outer coding are treated as the message bits for the inner coding. Hence, the average number of ATM cells for a slice is equal to $\lceil \overline{\text{CSlice}}/m \rceil (= \overline{n}_{\text{cell}})$, where $\lceil x \rceil$ denotes the smallest integer which is greater than x. As a result, $\overline{\text{Code}}_{\text{in}} = (255 - m) \times \overline{n}_{\text{cell}}$ and $\overline{\text{CATMh}} = 31 \times \overline{n}_{\text{cell}}$, where $m = 215$ (I-frame) or 223 (P-frame) or 231 (B-frame). Therefore, the expression of (2) becomes

$$\overline{R}_c \approx \frac{\overline{\text{Slice}}}{\left\{ \overline{\text{CSlice}} + [(255 - m) + 31] \times \left\lceil \frac{\overline{\text{CSlice}}}{m} \right\rceil \right\}} \tag{3}$$

where $m = 215$ or 223 or 231.

Since $\overline{\text{Slice}}$ is a fixed value independent of outer coding scheme, the maximization of $\overline{R}_c$ then becomes the minimization of $\overline{\text{CSlice}}$. The expression of $\overline{\text{CSlice}}$ for MPEG-2 in 4:2:0 mode is given by

$$\begin{aligned} \overline{\text{CSlice}} = {} & \overline{\text{CSliceh}} + \overline{\text{CMBh}} \times \overline{n}_{\text{MB}} \\ & + \overline{\text{CDC}}_Y \times \overline{n}_Y + \overline{\text{CDC}}_U \times \overline{n}_U \\ & + \overline{\text{CDC}}_V \times \overline{n}_V + \overline{\text{AC}} \quad \text{for I-frames} \end{aligned} \tag{4}$$

or

$$\begin{aligned} \overline{\text{CSlice}} = {} & \overline{\text{CSliceh}} + \overline{\text{CMBh}} \times \overline{n}_{\text{MB}} \\ & + \overline{\text{CMV}} \times \overline{n}_{\text{mv}} + \overline{\text{CDC}}_Y \times \overline{n}_Y \\ & + \overline{\text{CDC}}_U \times \overline{n}_U + \overline{\text{CDC}}_V \times \overline{n}_V + \overline{\text{AC}} \\ & \text{for P- or B-frames} \end{aligned} \tag{5}$$

where $\overline{\text{CSliceh}}$ is the average number of bits in a coded slice header using outer coding. $\overline{\text{CMBh}}$ denotes the average number of bits in a coded MB header, and $\overline{n}_{\text{MB}}$ is the average number of MB's in a slice. $\overline{\text{CDC}}_X$ denotes the average number of bits in the coded dc values of X-block and $\overline{n}_X$ represents the average number of X-blocks in a slice, where $X = Y$ or U (C_b) or V (C_r). $\overline{\text{CMV}}$ is the average number of bits in a coded motion vector and $\overline{n}_{\text{mv}}$ is the average number of motion vectors in a slice. Note that the above parameters are encoded using outer coding scheme only. Meanwhile, $\overline{\text{AC}}$ denotes the average number of bits belonging to the low priority AC coefficients in a slice without outer coding.

B. Adaptive Code Combining Strategy for Outer Code Selection

Two typical MPEG-2 videos are considered in the design of outer code selection. They are Flower Garden with a high average bit rate of 3 Mbits/frame and Table Tennis with a medium average bit rate of 1.5 Mbits/frame. Figs. 3 and 4 show the data distributions for DC values in Y-blocks, U-blocks, and V-blocks belonging to I-frames of Flower Garden and Table Tennis, respectively. Observing those data distributions, it is found that most of the high-priority data are distributed over a small number of bits. From Figs. 3 and 4, the maximum number of bits in DC_Y (DC values in Y-block) is 20. However, the probability of DC_Y less than 7 bits is 0.825 for Table Tennis or 0.569 for Flower Garden. Moreover, $\Pr\{\text{DC}_Y \leq 11 \text{ bits}\} = 0.978$ (Table Tennis), 0.969 (Flower Garden). In other words, most of DC_Y's are distributed over the range of

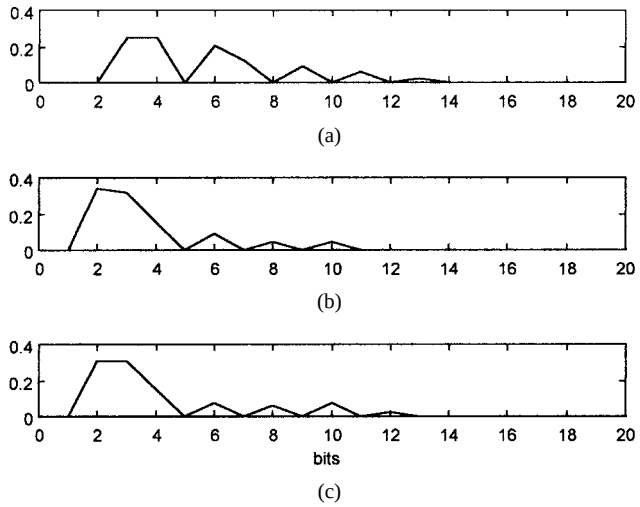

Fig. 3. Data distribution of DC coefficients in (a) Y-block, (b) U-block, and (c) V-block belonging to the I-frame of Table Tennis.

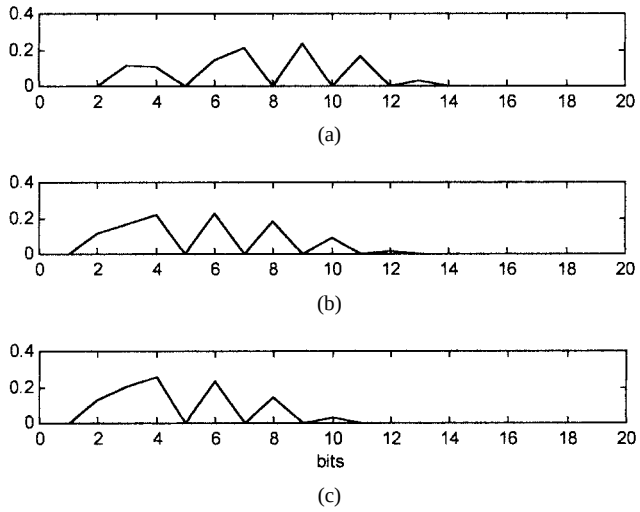

Fig. 4. Data distribution of DC coefficients in (a) Y-block, (b) U-block, and (c) V-block belonging to the I-frame of Flower Garden.

[0,11]. Based on the above observation, an adaptive code combining scheme is proposed to achieve the optimal outer code selection according to the statistical characteristics of MPEG source coding. This combining strategy is quite similar to the concept of Huffman source coding. Two basic shortened BCH codes of (7,4) and (15,7) play an important role in the code combining scheme in order to minimize the code overhead and also to provide good protection with reasonable delay. The following procedure for encoding DC_Y in an I-frame is treated as a typical example for code combining: 1) if $1 \leq \mathrm{DC}_Y \leq 4$ bits, use BCH(7,4) to encode DC_Y; 2) if $5 \leq \mathrm{DC}_Y \leq 7$, use BCH(15,7) to encode it; 3) if $8 \leq \mathrm{DC}_Y \leq 11$ bits, use BCH(7,4) + BCH(15,7) to encode it; 4) if $12 \leq \mathrm{DC}_Y \leq 14$ bits, use 2 × BCH(15,7) to encode it; 5) if $15 \leq \mathrm{DC}_Y \leq 18$ bits, use BCH(7,4) + 2 × BCH(15,7) to encode it; and 6) if $19 \leq \mathrm{DC}_Y \leq 20$ bits, use 2 × BCH(7,4) + 2 × BCH(15,7) to encode it. The probability for each data range can be found as : 1) $\Pr\{1 \leq \mathrm{DC}_Y \leq 4\} = 0.503$ (Table Tennis), 0.25 (Flower Garden); 2) $\Pr\{5 \leq \mathrm{DC}_Y \leq 7\} = 0.322$, 0.354; 3) $\Pr\{8 \leq \mathrm{DC}_Y \leq 11\} = 0.153$, 0.400; 4) $\Pr\{12 \leq \mathrm{DC}_Y \leq 14\} = 0.021$, 0.030; 5) $\Pr\{15 \leq \mathrm{DC}_Y \leq 18\} = 5.536 \times 10^{-4}$, 4.850×10^{-4}; 6) $\Pr\{19 \leq \mathrm{DC}_Y \leq 20\} = 1.1 \times 10^{-8}, 2.1 \times 10^{-8}$. Therefore, the average number of bits in the BCH outer-coded DC_Y belonging to an I-frame becomes $\overline{\mathrm{CDC}_Y} = 12.3675$ for Table Tennis or 16.5320 for Flower Garden. Similarly, the same BCH outer code combining can be applied to DC values in both the U- and V-blocks belonging to an I-frame. Hence, $\overline{\mathrm{CDC}_U} = 9.1779$ (Table Tennis), 13.188 (Flower Garden), $\overline{\mathrm{CDC}_V} = 10.148$, 11.573. $\overline{n}_Y, \overline{n}_U, \overline{n}_V$ are found to be 88, 22, 22 for either Table Tennis or Flower Garden. A combining of 6 × BCH(15,7) is used to encode a fixed 38-bit slice header belonging to an I-frame with high FEC protection. Similarly, a fixed 2-bit MB header is protected by BCH(7,4). As a result, $\overline{\mathrm{CSlice}} = 90$ and $\overline{\mathrm{CMBh}} = 7$. In addition, $\overline{n}_{MB}$ equals 22 for both Table Tennis and Flower Garden, and $\overline{\mathrm{AC}} = 12\,096.49$ for Table Tennis or 22 141.772 for Flower Garden. From (4), $\overline{\mathrm{CSlice}} = 13\,854.002$ for Table Tennis or 24385.409 for Flower Garden. Moreover, the average code rate for ATM cells generated from an I-frame is computed by (3). It yields $\overline{R}_{c,I} = 0.6957$ for Table Tennis or 0.7388 for Flower Garden. In addition, the data distribution for high priority data in either P- or B-frame belonging to either Flower Garden or Table Tennis can be found in [29]. It is found that their high priority data are also distributed over a small number of bits. For P- and B-frames, the same BCH outer code combining scheme is applied to their high priority data according to their data distribution. However, a combining of BCH(15,7) + 2 × BCH(31,16) is applied to the 38-bit slice header belonging to either P- or B-frame with a medium FEC protection. This leads to $\overline{\mathrm{CSlice}} = 77$. The average code rate for ATM cells generated from either P- or B-frame is found to be $\overline{R}_{c,P} = 0.755\,12$ (Table Tennis) or 0.766 65 (Flower Garden), or $\overline{R}_{c,B} = 0.650\,94$ (Table Tennis) or 0.754 85 (Flower Garden). In the near future, a class of rate compatible punctured convolution codes (RCPC's) as well as turbo codes will be considered in the design of the inner coding for MPEG videos in order to achieve the better FEC code performance, where turbo codes are, in essence, parallel concatenated convolutional codes which have been shown to perform near the capacity limit on fully interleaved fading channels [30]. Moreover, we will concatenate our proposed BCH outer code combining scheme with either RCPC or turbo inner code [31] to further reduce the BER floor.

IV. Transmission of MPEG-2 Videos over ATM-Based Multicode CDMA Mobile Communication Networks

In the near future, the third-generation mobile communication will allow high mobility users to access video information stored at various network sites. The multicode CDMA seems one of the major technologies [1], [9], [10] for supporting video services in the third-generation

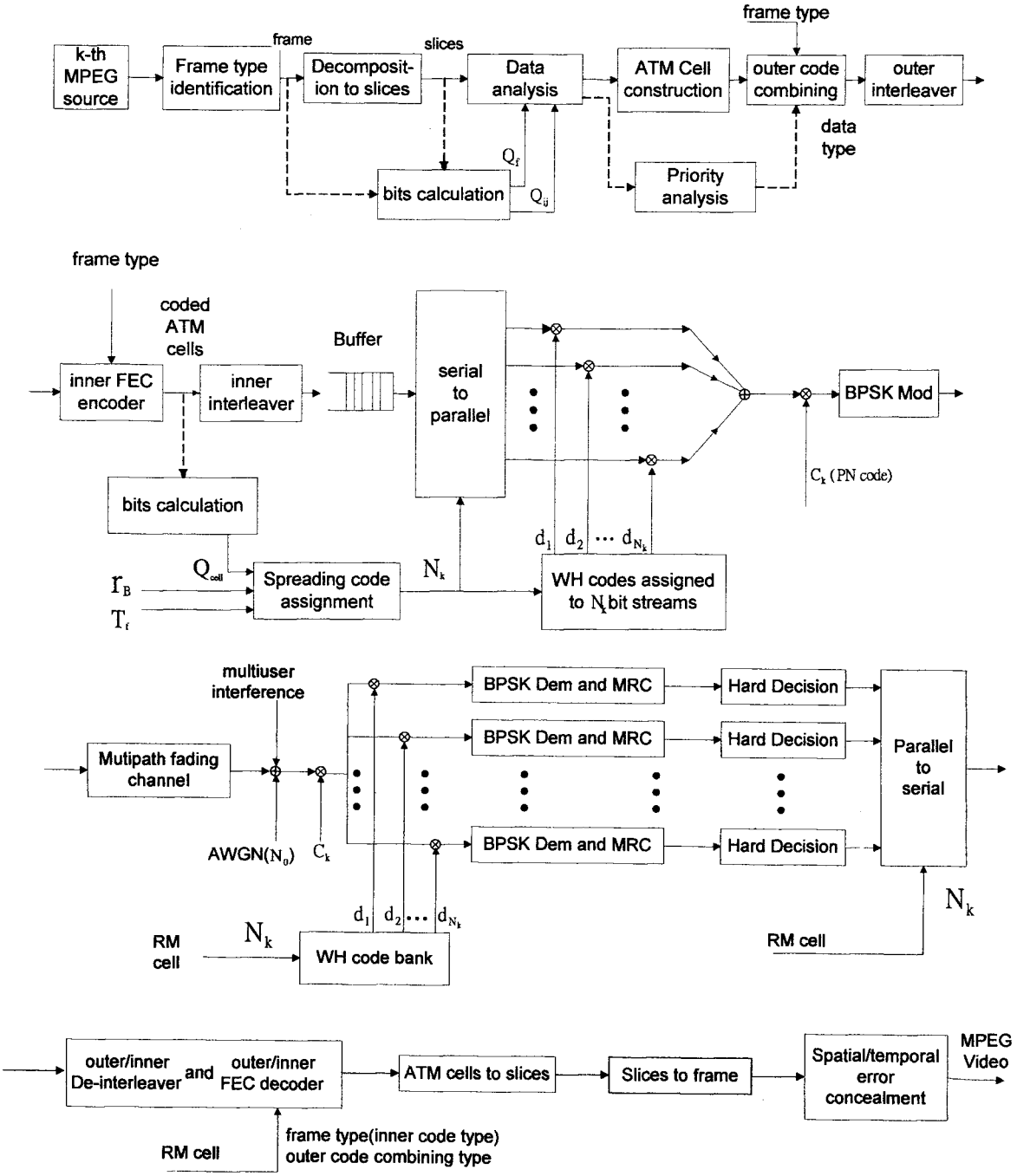

Fig. 5. Overall schematics of multiple MPEG video transmission via ATM-based multicode CDMA system where RM cell contains N_k, frame type, and outer code combining type.

system. In this paper, we are trying to propose a generic multicode CDMA system for providing the transmission of multiple MPEG-2 videos via a wireless ATM network. Fig. 5 shows this concept. For the kth MPEG source, the system first identifies the frame type at a specific time instant, and the frame is then decomposed into a number of slices. A data priority analysis is applied to each slice for the construction of wireless ATM cells. Moreover, an outer FEC code proposed in Section III is applied to the high-priority payload according to the priority analysis. Moreover, an inner FEC code is used to protect the outer-coded high-priority data twice and the remaining low-priority data with regard to the importance of the frame type in the temporal domain. Since the traditional CDMA system may not be sufficient to accommodate the transmission of multiple high bit-rate MPEG videos via a narrow-band mobile channel, a multicode CDMA technique is proposed to overcome this difficulty. In the multicode CDMA system, when the kth MPEG needs N_k times the basic transmission rate, it converts the original high bit-rate bit stream using a multiplexer or serial-to-parallel converter into N_k basic rate streams, encodes each with a different spreading code, modulates them with a different Walsh modulator, and superimposes them before upconverting for

mobile transmission. In other words, each spreading code in the multicode CDMA carries a data stream with a basic rate r_B. N_k spreading codes in parallel will provide a single user with N_k times the basic rate capability. Note that each MPEG admitted into the system has a primary PN code assigned to it. These PN codes are not orthogonal between different MPEG users. To avoid the self-interference that a MPEG user employing multiple codes may incur, the multiple codes to/from one user should be made orthogonal. If c_k is the primary PN code assigned to the kth MPEG with a basic transmission bit rate r_B, N_k new concatenated spreading codes, a_{km}'s can be derived by $a_{km} = c_k \times d_m$, $1 \leq m \leq N_k$, where d_m is the mth orthogonal code, and $d_l \perp d_m$ if $l \neq m$. It should be mentioned that the actual value of N_k depends on the frame type, frame period, basic transmission rate, desired cell loss rate (CLR), and total number of bits in all the coded ATM cells. In Section V, a spreading code assignment mechanism is proposed to determine an appropriate value of N_k which is able to achieve both the higher transmission capability and better received picture quality. Due to the orthogonality requirement, the maximum number of orthogonal codes per user is the ratio N_c between the channel chip rate and the Walsh modulator output rate. N_c is termed as the spreading sequence length. Hence, $N_k \leq N_c$. The above coding strategy is called the subcode concatenated scheme that orthogonal sequences are concatenated with a PN sequence to increase the randomness of the orthogonal sequence. The binary orthogonal sequences used in this paper were the well-known Walsh–Hadamard (WH) codes which have zero cross correlation at zero time delay. They are used when synchronization of transmission can be maintained. Unfortunately, the multipath fading in a cellular radio environment introduces nonzero time delays that destroy the orthogonality between Walsh–Hadamard (WH) codes. Fong *et al.* [7] showed that a sufficiently long PN sequence is concatenated with WH codes to randomize and eliminate their unsatisfactory and inhomogeneous behavior at nonzero time delays. The long PN sequence may be chosen as either m-sequence or Gold sequence. Before transmitting the ATM cells, an RM cell containing the frame header, the value of N_k, and the resource management information is sent to the desired mobile receiver. Thus, the receiver is able to demodulate the N_k bit streams. Finally, spatial/temporal error concealment techniques are proposed to improve the received image quality.

A. Multicode CDMA Transmitter Model with Concatenated Orthogonal/PN Spreading Code Scheme

For K MPEG videos transmitted over a mobile channel, each of them is divided into $N_k(t)$ parallel data streams (virtual channels) for user k at time t, where a specific WH code is assigned to each virtual channel. The value of $N_k(t)$ is dynamically determined by a code assignment mechanism discussed in the next section. For simplicity, $N_k(t)$ is assumed to be a constant N_{kj_k} in the j_kth time interval $I_{kj_k} = [T_{kj_k}, T_{k,j_k+1}]$, i.e., $N_k(t) = N_{kj_k}$ for $t \in I_{kj_k}$. Hence, the total number of WH codes assigned to all the K users in the new time interval I_j is $M = \Sigma_{k=1}^{K} N_{kj_k}$, where I_j denotes the jth intersection interval of the time intervals for all the K MPEG's, i.e., $I_j = \bigcap_{k=1}^{K} I_{kj_k}$. Usually, $T_f = T_{k,j_k+1} - T_{k,j_k}$ is a fixed value called the frame period. Note that WH codes assigned to different users with different PN codes may be identical. It should be mentioned that the above arguments are valid when each user has a continuous MPEG video presentation. However, this assumption may not be true since some users may not have MPEG videos during a specific time interval, i.e., I_{kj_k}. To tackle this difficulty, the value of N_{kj_k} for this particular interval is set to zero. Therefore, the above argument becomes valid again. For simplicity, we assume that each of the K MPEG's has its corresponding picture frames during I_j. The transmitting binary phase shift keying (BPSK) signal $s_{km}(t)$ of the mth data stream (virtual channel) belonging to the kth MPEG during the jth time interval I_j is expressed as

$$s_{km}(t) = \sqrt{2P} a_{km}(t) b_{km}(t) \cos(\omega_c t + \theta_{km}) \quad t \in I_j, \quad 1 \leq m \leq N_{kj} \leq N_c, 1 \leq k \leq K \tag{6}$$

where P is the transmission power of the base station, θ_{km} is the random phase angle, uniformly distributed between zero and 2π, introduced by the modulator, and $b_{km}(t)$ is the data signal which consists of a sequence of rectangular pulses of duration T, i.e.,

$$b_{km}(t) = \sum_{i=-\infty}^{\infty} b_{km}^{i} \Pi_T(t - iT) \tag{7}$$

where $b_{km}^{(i)} \in \{1, -1\}$ and $\Pi_T(t)$ is a unit pulse function of duration T. The concatenated spreading code $a_{km}(t)$ can be expressed as

$$a_{km}(t) = \sum_{i=-\infty}^{\infty} a_{km}^{(i)} \Pi_{T_c}(t - iT_c) \tag{8}$$

where $a_{km}^{(i)} \in \{-1, 1\}$ is the concatenated spreading sequence which is equal to the product of a PN sequence $c_k^{(i)} \in \{-1, 1\}$ used by the kth user and a WH code sequence $d_m^{(i)} \in \{-1, 1\}$ assigned to its mth virtual channel. The duration of each data bit is T, while the duration of each chip in the spreading code is T_c. The number of chips per bit is $N_c = T/T_c$, where N_c is an integer. The period of the WH code sequence $d_m^{(i)}$ is equal to the processing gain N_c. The long PN sequence $c_k^{(i)}$ has a period N_{PN} that is much greater than N_c. Moreover, N_{PN} and N_c are chosen to be relatively prime so that every possible chip of the PN sequence can occur at the beginning of some data bit. As a result, the total signal transmitted to K users is

$$s(t) = \sum_{k=1}^{K} \sum_{m=1}^{N_{kj}} s_{km}(t), \qquad t \in I_j = \bigcap_{k=1}^{K} I_{kj}. \tag{9}$$

B. Mobile Radio Channel Model

The Rayleigh multipath fading model is the general accepted channel model for mobile communications [22]. In this paper, we adopted the Rayleigh fading model for performance analysis in our multicode CDMA system. The channel impulse response for the mth virtual channel assigned to the kth user is given by

$$h_{km}(t) = \sum_{l=1}^{L_{km}} \beta_{lkm}\delta(t-\tau_{lkm})e^{j\phi_{lkm}} \quad t \in I_j, \quad 1 \le m \le N_{kj}, \quad 1 \le k \le K \tag{10}$$

where β_{lkm} is the lth Rayleigh distributed random path gain, ϕ_{lkm} is the lth random path phase, uniformly distributed between zero and 2π, and τ_{lkm} is the lth uniformly distributed random delay ranging from zero to one data bit period T. $\delta(t)$ represents the unit impulse function. L_{km} denotes the number of resolvable multipaths for the mth virtual channel assigned to user k. In addition, it should be mentioned that these channel parameters vary with the transmitter–receiver distance. It may be shown that $\overline{\beta}^2_{lkm} = \overline{\beta}^2_{lk1} = \overline{\beta}^2_{lk}$ and $L_{km} = L_{k1} = L_k$ for $1 \le m \le N_{kj}$ since all the parallel virtual channels introduced by the same user are transmitted over the same propagation environment between the transmitter and receiver, and then would have identical channel characteristics, where $\overline{x}^2$ denotes the variance of a random variable x.

C. Receiver Model

The received signal at the input to the mobile receiver is given by

$$\begin{aligned} r(t) &= \mathrm{Re}\left\{\int_{-\infty}^{\infty} h_{km}(\tau)\tilde{s}_{km}(t-\tau)\exp(j\omega_c t)\,d\tau\right\} + n(t) \\ &= \sqrt{2P}\sum_{k=1}^{K}\sum_{m=1}^{N_{kj}}\sum_{l=1}^{L_{km}} \beta_{lkm}a_{km}(t-\tau_{lkm})b_{km} \\ &\quad \cdot (t-\tau_{lkm})\cos(\omega_c t + \varphi_{lkm}) + n(t) \\ \varphi_{lkm} &= -\omega_c\tau_{lkm} + \phi_{lkm} + \theta_{lkm} \end{aligned} \tag{11}$$

where $\tilde{s}(t)$ is the complex envelope of $s(t)$, $\mathrm{Re}\{\cdot\}$ denotes the real part of complex number, and $n(t)$ is a white Gaussian noise with two-sided power spectral density $N_0/2$.

For simplified analysis, the first virtual channel assigned to the first user is chosen as the reference for calculating the probability of error of its data symbol $b_{11}^{(j)}$ in the jth sampling time interval $I_s^{(j)} = [(j-1)T, jT]$. The receiver is able to coherently recover the carrier phase φ_{lkm} and τ_{klm} locking to the lth path as a reference path between the reference transmitter and its corresponding receiver. All other paths constitute interference. That is, we assume without loss of generality that $\varphi_{l11} = 0$ and $\tau_{l11} = 0$. The envelope of the output of the optimum BPSK demodulator at the jth sampling time instant $(t = jT)$ is denoted by $Y_{11}^{(j)}$ and can be expressed as

$$\begin{aligned} Y_{11}^{(j)} &= \int_{(j-1)T}^{jT} r(t)a_{11}(t)\cos(\omega_c t)\,dt + \nu \\ &= \beta_{l11}\sqrt{\frac{PT^2}{2}}b_{11}^{(j)} + Int_1 + Int_2 + Int_3 + \nu \\ I_s^{(j)} &\subseteq I_j = \bigcap_{k=1}^{K} I_{kj} \end{aligned} \tag{12}$$

where

$$\nu = \int_{(j-1)T}^{jT} n(t)a_{11}(t)\cos(\omega_c t)\,dt. \tag{13}$$

Int_1 is the intra multi-user interference (self-interference) indicating the interference introduced by the other virtual channels belonging to the same reference user, Int_2 is the intra multipath interference, and Int_3 denotes the inter multi-user interference. It should be noted that the orthogonality of the concatenated spreading codes eliminates the intra multi-user interference (self-interference) [10]. This leads $Int_1 = 0$.

D. Calculation of Average CLR

This wireless ATM cell is transmitted over the wireless CDMA link. Assuming that bit synchronization and cell synchronization have been achieved, the mobile receiver first decodes the ATM header. If the cell is successful, the receiver then decodes the payload. There are two major factors that cause wireless networks to discard cells. One is bit errors in the header due to the multipath fading, interference, and channel noise. The other is buffer overflow in multiplexing or cross-connecting equipment. The cell loss process due to buffer overflow can be approximated by a two-state Markov chain called Gilbert model [23]. Here, for simplicity, we only consider the cell loss due to the bit errors in the header. Usually, a single cell loss may cause a loss of a amount of image data and results in a high degradation of picture quality. Hence, the CLR is regarded as the major performance index used to evaluate the quality of received picture. For the simplified derivation of the CLR, the Gaussian assumption is to take all the self-interference, intra multipath interference, and inter multi-user interference terms as Gaussian noise. Reference [29] has shown that the average value of half the signal-to-noise plus interference power ratio becomes

$$\overline{\gamma}_b = \left[\frac{2M}{3N_c}\left(\eta - \frac{N_{1j}}{M}\right) + \frac{N_0}{\overline{E}_b}\right]^{-1} \tag{14}$$

where $\overline{E}_b (= \overline{\beta}_l^2 PT)$ represents the received signal energy per bit via the lth path (reference path), $M = \Sigma_{k=1}^{K} N_{kj}$, and $\eta = \Sigma_{q=1}^{L}(\overline{\beta}_q^2/\overline{\beta}_l^2)$. Note that η is always greater than one. For simplicity, assume that the path gains for all the virtual channels in the same user are independent identically distributed (i.i.d.), i.e., $\overline{\beta}_q^2 = \overline{\beta}^2$, $1 \le q \le L$. Thus the value of η is identical to L, i.e., $\eta = L$. Proakis [22] showed that the bit error rate (BER) for a receiver with maximal ratio

combining (MRC) of order L_d can be expressed as a form in terms of $\overline{\gamma}_b$

$$p_e = \left(\frac{1-\mu}{2}\right)^{L_d} \times \sum_{s=0}^{Ld-1} \binom{L_d - 1 + s}{s} \left(\frac{1+\mu}{2}\right)^s \quad \text{for MRC of order } L_d. \tag{15}$$

In (15), for MRC, the quantity $\overline{\gamma}_b$ represents the average signal-to-noise ratio per combined path, and $\mu = \sqrt{\overline{\gamma}_b/1+\overline{\gamma}_b}$.

Since a BCH code of (31,16,3) is proposed to protect the 16-bit compressed ATM header, the CLR is computed by

$$\mathrm{CLR} = \sum_{i=4}^{31} \binom{31}{i} (1-p_e)^{31-i} p_e^i. \tag{16}$$

V. Frame Interleaving Techniques for Multi-User Traffic Regulation

Fig. 6 shows the bit-rate trace which is a bitcount observed frame-by-frame in a segment (frames 1-150) in Flower Garden. The main peaks on the 360-kbit range, correspond to I-frames, while the second peaks, on the 220–310-kbit, are P-frames; the frames on the 63-kbit range are B-frames. The bit-rate trace of Table Tennis is presented in Fig. 7. Its I-frames, P-frames, and B-frames are on the range of 193, 116, and 21 kbit, respectively. The total bit count of this two-user video transmission becomes 553 kbit when the I-frames of both Flower Garden and Table Tennis are transmitted to mobile receiver simultaneously. Due to the transmission rate limitation of mobile channel, it is difficult to carry such multiple high bit-rate I-frames over a narrow-band mobile channel within a short frame time period ($1/30 \sim 1/10$ s) simultaneously. On the other hand, the bit-count of the two-user video transmission becomes extremely low (84 kbit) when both low bit-rate B-frames are transmitted at the same time. This rapidly VBR characteristics seems a weakness to the transmission of multiple MPEG videos via a CBR mobile channel. To tackle this difficulty, a frame interleaving strategy is proposed to avoid the simultaneous appearance of multiple high bit-rate frames and then regulate the total multi-user traffic. An optimal frame interleaving pattern can be found by minimizing the total multi-user traffic subject to an inter-user time delay constraint of T_d. In this paper, both the GOP and n_P of each MPEG video are assumed to be identical to 6, where GOP and n_P are the distance between I-frames and the distance between P-frames, respectively. Two typical MPEG videos of GOP $= 6$ and $n_P = 6$ are Flower Garden and Table Tennis. To illustrate the concept of frame interleaving, we consider an example of five MPEG videos of GOP $= 6$ and $n_P = 6$ under a reasonable inter-MPEG delay constraint of $T_d = 3T_f$. The optimal frame interleaving pattern for these five MPEG videos is given at the bottom of the page.

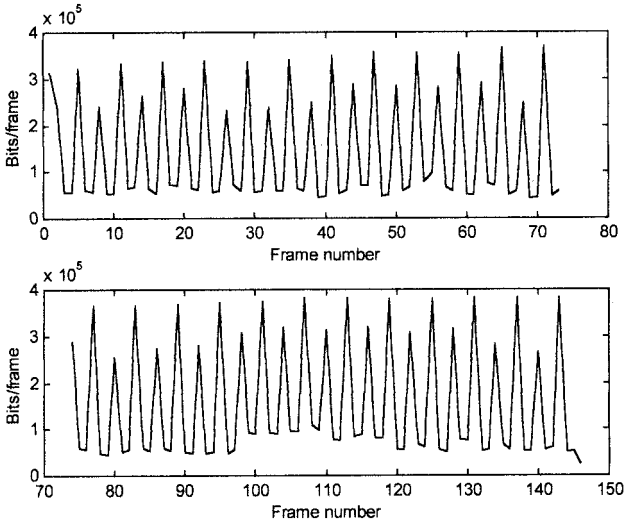

Fig. 6. Bit-rate trace for Flower Garden.

In the optimal interleaving pattern, the lowest average bit-rate MPEG video is given to MPEG 1 and the highest average bit-rate MPEG video is assigned to MPEG 5. The nth MPEG is delayed by a time interval of n frame periods with respect to MPEG 1 in order to avoid the simultaneous appearance of multiple high bit-rate frames, $2 \le n \le 4$. However, due to the delay constraint of $T_d = 3T_f$, two I-frames may appear in both MPEG 1 and MPEG 5 at the same time. Therefore, at steady state (after three frame periods), this leads to six frame combinations, (P,B,B,I,P), (B,P,B,B,B), (B,B,P,B,B), (I,B,B,P,I), (B,I,B,B,B), and (B,B,I,B,B), and the frame combination with a maximum five-user bit rate in the proposed frame interleaving is (I,B,B,P,I), where the ith component represents a specific frame type of the ith MPEG, where $1 \le i \le 5$. There are two high bit-rate I-frames, one medium bit-rate P-frame, and two low bit-rate B-frames belonging to the maximum five-user bit-rate frame combination which are much better than five high bit-rate I-frames that appear in the transmission of five MPEG videos simultaneously. It should be noted that these six frame combinations may be reduced to four frame combinations when these five MPEG videos have an identical bit-rate for each of their I-, P-, and B-frames. The concept of frame interleaving can be extended to a more general case. The optimal frame

Time:	t_1	t_2	t_3	t_4	t_5	t_6	t_7	t_8	t_9	t_{10}	t_{11}	t_{12}	t_{13}	t_{14}	t_{15}	·	·	·
MPEG-1:	I	B	B	P	B	B	I	B	B	P	B	B	I	B	B	·	·	·
MPEG-2:		I	B	B	P	B	B	I	B	B	P	B	B	I	B	·	·	·
MPEG-3:			I	B	B	P	B	B	I	B	B	P	B	B	I	·	·	·
MPEG-4:				I	B	B	P	B	B	I	B	B	P	B	B	·	·	·
MPEG-5:	I	B	B	P	B	B	I	B	B	P	B	B	I	B	B	·	·	·

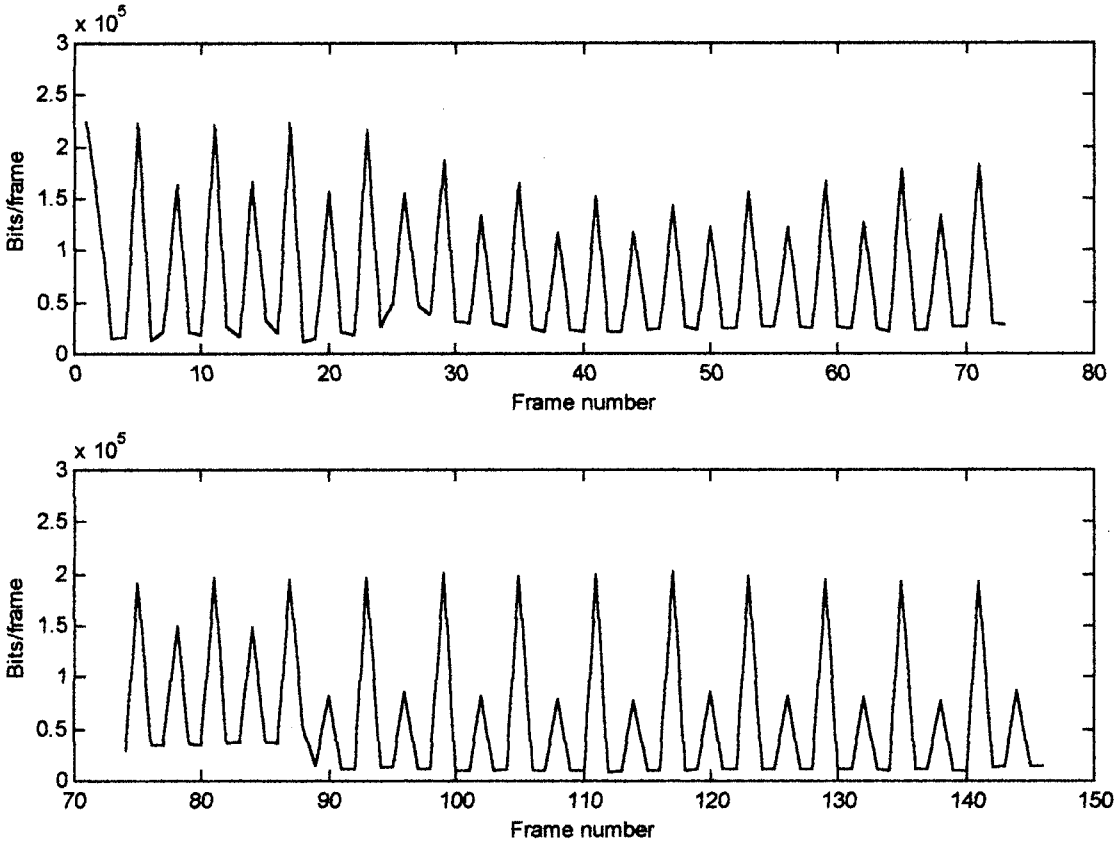

Fig. 7. Bit-rate trace for Table Tennis.

interleaving of K MPEG videos with different GOP and n_P can be obtained by minimizing the following performance index called the effective bandwidth for total K multiplexed MPEG video streams [32] using the simulated annealing algorithms:

$$BW_{\text{eff}}(\boldsymbol{t}_d) = \max_{t>0}\left(\sum_{i=1}^{K}\xi_i(t-t_{d,i})\right) \quad \text{subject to } 0 \le t_{d,i} \le T_d, 1 \le i \le K \qquad (17)$$

where $\xi_i(t)$ denotes the bit-rate trace (traffic envelope) for the ith MPEG video stream, $\boldsymbol{t}_d = [t_{d,1}, t_{d,2}, \ldots, t_{d,K}]$ referred as the time delay arrangement vector, completely specifies the synchronization structure for the K streams, $t_{d,i}$ is the time delay for the ith MPEG stream, and K is any positive integer.

VI. Dynamic Spreading Code Assignment for Multiple MPEG Video Services

The spreading code assignment mechanism is responsible for assigning an appropriate number of WH codes frame by frame for every MPEG video in each frame time period so that the received picture quality of each MPEG video is guaranteed with a CLR value less than the maximum allowable CLR. For example, it is found that the average number of ATM cells for each of I-, P-, and B-frames belonging to both typical MPEG videos Flower Garden and Table Tennis according to the concatenated channel coding is in the order of $O(10^2) \sim O(10^3)$. For example, the average number of ATM cells for an I-frame is 1.41×10^3 for Flower Garden or 9.75×10^2 for Table Tennis. The maximum allowable cell loss rate is then set to be in the order of $O(10^{-3}) \sim O(10^{-2})$ if the allowable average number of cell losses in a frame is in the order of $O(1)$. The picture degradation due to these cell losses can be eliminated by using the spatial and temporal error concealment technique proposed in Section VII. From (16), it is known that the maximum allowable CLR for each frame depends essentially on η, frame combination, and the number of WH codes assigned to each frame in a specific frame combination. On the contrary, it is desired to obtain the appropriate maximum WH code number assigned to each frame that is able to achieve its maximum allowable CLR. For ease of analysis, it is assumed that all the MPEG videos with an identical medium bit-rate trace are transmitted over a typical indoor multipath fading channel [25] with $\eta = 4$ and $(\overline{E}_b/N_0) = 25$ dB. Hence, the number of WH codes assigned to each frame belonging to any one of the above MPEG videos with an identical bit-rate trace is assumed to be identical. This medium bit-rate MPEG video may be chosen as Table Tennis. In each frame interleaving scheme, the maximum multi-user bit-rate frame combination belonging to the optimal frame interleaving will play an important role in the determination of maximum allowable WH code number assigned to each frame. There is no general method to determine such numbers, only the heuristic method. It is found that the

maximum K-user bit-rate frame combination belonging to the optimal frame interleaving contains only the I- and B-frames when the number of users, K is equal to either two or three and the inter-MPEG delay constraint is $T_d = 3T_f$. In this case, there are one I-frame and $(K-1)$ B-frames involved in the combination, where $2 \le K \le 3$. Therefore, the CLR is a function of two integer variables, N_I and N_B, which are the numbers of WH codes assigned to I- and B-frames belonging to any one MPEG video, respectively. The cell loss rate for I-frame, i.e., CLR_I due to $(K-1)$ interfering B-frames is characterized by the following half the signal-to-noise plus interference power ratio:

$$\overline{r}_{b,I} = \left\{ \frac{2}{3N_c}[3N_I + 4(K-1)N_B] + 0.0031622 \right\}^{-1} \tag{18}$$

In contrast to CLR_I, the cell loss rate for a specific B-frame, i.e., CLR_B, due to one interfering I-frame and $(K-2)$ interfering B-frames is characterized by

$$\overline{r}_{b,B} = \left\{ \frac{2}{3N_c}[3N_B + 4N_I + 4(K-2)N_B] + 0.0031622 \right\}^{-1}. \tag{19}$$

Next, it is desired to determine the appropriate values for both N_I and N_B which are able to quarantee both CLR_I and CLR_B be in their respective maximum allowable ranges. The average number of WH codes assigned to a specific frame can be estimated by

$$\overline{N} = \left\lceil \frac{\overline{Q}_f}{r_B \overline{R}_c T_f} \right\rceil \tag{20}$$

where $\overline{Q}_f$ denotes the average number of bits in a specific frame, T_f is set to be $\frac{1}{10}$ s and $r_B = 64$ kbit/s [10]. In Section III, for Table Tennis, it is found that $\overline{R}_c$ equals 0.6957 for an I-frame or 0.755 12 for a P-frame or 0.650 94 for a B-frame. In addition, the actual value of $\overline{Q}_f$ is obtained to be 1.9274×10^5 bits/frame for an I-frame or $1.161\,55 \times 10^5$ bits/frame for a P-frame or 2.0737×10^4 bits/frame for a B-frame. Therefore, the resulting average WH code numbers become $\overline{N}_I = 43$, $\overline{N}_P = 24$, and $\overline{N}_B = 5$ that are used to determine the rough estimate for the operating range of maximum allowable WH code number for each frame. From the above discussion and (15)–(17), it is found that $N_{\max,I} = 50$, and $N_{\max,B} = 10$ are able to guarantee that the CLR's for both I- and B-frames are in the order of 10^{-3} when $K = 2$. Moreover, the average number of ATM cells for each frame in Table Tennis is 9.75×10^2 for an I-frame, or 5.4×10^2 for a P-frame, or 1.2×10^2 for a B-frame according to the ATM cell generation method proposed in Section III. This leads to almost one cell loss in each frame. By the similar analysis, $N_{\max,I}$ and $N_{\max,B}$ become 45 and 6, respectively, in order to guarantee the reasonable CLR for eithe I- or B-frame when K becomes three. When K is greater than three, a P-frame will appear in the maximum four-user bit-rate frame combination, i.e., (I,B,B,P) if $K = 4$, or two I-frames and one P-frame appear in the maximum five-user bit-rate frame combination (I,B,B,P,I) if $K = 5$. When K becomes larger, the total number of WH codes assigned to those frames also becomes larger and then creates larger interference to each other. In order to achieve the reasonable CLR for each frame, it is possible to abandon some low-priority data of the least important frames, (B- or P-frames), so that the picture quality is still maintained. For example, the picture quality for a B-frame in Table Tennis is still at the decoded video peak signal to noise ratio (PSNR) performance of $\mathrm{PSNR}_Y = 33.602$, $\mathrm{PSNR}_U = 39.343$, and $\mathrm{PSNR}_V = 41.254$ when 60% of AC coefficients have been abandoned. This results in $N_B = 3$. Similarly, the picture quality for a P-frame is at the performance of $\mathrm{PSNR}_Y = 35.151$, $\mathrm{PSNR}_U = 39.749$, and $\mathrm{PSNR}_V = 41.912$ when 40% of AC coefficients have been abandoned. Thus, the value of N_P is decreased from 24 to 17. One may abandon more low-priority data when K becomes larger. Therefore, both the desired CLR and picture quality for each frame can be achieved. Note that the above analysis for the case of multiple MPEG video streams with an identical bit-rate trace can be extended to a more general case. For example, the bit-rate traces for multiple MPEG videos may be extremely different. The analysis to the general case can be found in Section VIII.

A. Spreading Code Assignment Mechanism

Since WH codes assigned to an MPEG video would create the interference to the other MPEG videos, this leads to a picture degradation in those MPEG videos. The limited maximum allowable number of WH codes is used to ensure the picture quality of all the MPEG videos within an acceptable level. Meanwhile, more WH codes also provide more virtual channels for transmission of multiple MPEG videos in order to carry all the image data or high-priority data to receivers within a short frame time period as much as possible. The tradeoff between picture quality and transmission capability seems a critical factor in determining an appropriate number of WH codes for each MPEG video. However, there is no general principle to justify this tradeoff. Our approach is based on the heuristic method. First, we should determine the optimal frame interleaving and its maximum multi-user bit-rate frame combination. Then, the maximum allowable WH code number, i.e., $N_{\max}$ for each frame is determined according to the analysis of CLR's discussed above. Thus, the maximum average message bits transmitted over $N_{\max}$ virtual channels within a frame period T_f is calculated by $\overline{Q}_{\max} = N_{\max} \times r_B \times T_f \times \overline{R}_c$. Let Q_f denote total number of bits in the frame of interest, and let Q_{ij} denote the number of bits in the jth macroblock belonging to slice i. The low-priority data of $\Delta Q = Q_f - \overline{Q}_{\max}$ bits should be abandoned according to priority bank if Q_f is greater than $\overline{Q}_{\max}$. In the meantime, the number of abandoned bits in the jth MB belonging to slice i is proportional to Q_{ij}, that is, $\Delta Q_{ij} = (Q_{ij}/Q_f) \times \Delta Q$. Hence all the slices have been recreated based on those new macroblocks. Thus, an outer/inner code combining scheme is applied to each slice,

and then to generate a number of coded ATM cells. The actual value of WH code number assigned to the frame is determined by total number of bits in all the coded ATM cells, frame period, and transmission bit rate. More details of assignment mechanism are described in the following algorithm:

Procedure

step 1 [Check whether the system is able to carry Q_f bits/frame within T_f ?]

If $\Delta Q \leq 0$, go to step 3, otherwise do the following step,

step 2 [Abandon the low-priority data in each MB]

i) Abandon ΔQ_{ij} low-priority bits in the ith MB belonging to slice j according to the priority bank

ii) Re-create each MB with the higher-priority bits: $Q_{ij} \leftarrow Q_{ij} - \Delta Q_{ij}$ and $Q_f \leftarrow \Sigma_i \, \Sigma_j \, Q_{ij}$

step 3 [Create the coded ATM cells]

i) Rearrange the slices based on the new MB's

ii) Choose the appropriate inner FEC for payload and add the coded cell header to the ATM cell

iii) By analyzing both the priority and statistical behavior of data, data bits of each slice are first packetized in the ATM adaptation layer (AAL), and then packed into the ATM cell according to the outer FEC code combing

step 4 [Spreading code assignment]

i)

$$\begin{aligned} Q_{\text{cell}} &= \text{total number of bits in all the coded ATM cells} \\ &= Q_f + (\text{no. of bits in all the coded} \\ &\qquad \text{ATM cell headers}) \\ &\quad + (\text{no. of bits in the outer/inner FEC overheads}) \end{aligned} \tag{21}$$

ii)

$$\begin{aligned} N &= \text{number of WH codes assigned to the frame} \\ &= \left\lceil \frac{Q_{\text{cell}}}{T_f r_B} \right\rceil. \end{aligned} \tag{22}$$

VII. Spatial and Temporal Error Concealment Techniques for MPEG-2 Video with Information Loss

Zhang and Lee [12] have shown that the MPEG-2 source coding algorithm is very sensitive to multipath fading and interference. For example, a single bit error in the ATM header (cell loss) will often result in loss of a whole image block, which could further cause consecutive block losses. Sometimes, a number of consecutive blocks may be destroyed when a single bit error occurs in either slice header or macroblock header or motion vector even the ATM cell is successful.

The cell discarding may also be caused by network congestion and buffer overflow [23]. Several methods have been proposed to minimize the effect of cell loss on the received image quality. These schemes include FEC coding with interleaving and error concealment using postprocessing methods [13]–[18]. In this paper, we consider the combination of these strategies. The two main cell loss resilience techniques described here are the spatial and temporal error concealment techniques. The spatial error concealment exploits the spatial redundancy in one picture. This technique is proposed for intracoded pictures, i.e., I-frame, where no motion information exists. Temporal error concealment makes use of the temporal redundancy in one sequence. It is devoted to intercoded pictures, i.e., P- and B-frames, because there exists some motion information. It should be mentioned that the spatial/temporal error concealment techniques are also applied to the recovery of information loss even the ATM cells are successful. For instance, a single bit error in the DCT coefficients may damage one block when the DCT coefficients of each block are coded using run-length and variable-length coding. Moreover, a number of subsequent blocks may be destroyed if a single bit error occurs in either macroblock header or slice header.

A. Multiresolution Multidirectional Interpolation for Spatial Error Concealment

Since lost blocks are often correlated with neighboring spatial blocks due to the correlation property of nature images, interpolation and surface fitting can be used to partially recover the lost information [13], [14]. However, such techniques are low-pass filtering in nature and tend to ignore high-frequency information such as edges and contours. Lee *et al.* [16] have proposed a fuzzy logic approach to recover the lost blocks with high frequency and yield the desired reconstructed picture quality. Meanwhile, this fuzzy loss recovery technique is too complicated for implementation. Therefore, a cost-effective multidirectional interpolation [15] is employed to conceal the lost block with high frequency, where the damaged block is surrounded by eight neighboring blocks of correctly received pixels. A voting classification mechanism operates on the eight neighboring correct blocks and determines which directions characterize the three strongest edges. A spatial interpolation is performed to create the recovered block for each direction separately. Those interpolation results are then mixed by averaging to obtain the final recovered block containing multiple interpolated edges. The determination of the directions for the strongest edges depends on extending edges presented in the neighboring blocks so that they pass through the damaged block. The direction classification for edges can be performed by Sobel gradient operator which is able to give accurate angle estimates.

The multidirectional interpolation works well when the angular direction of edge is near to one of eight directional categories. However, this method becomes invalid when the edge direction is not close to any directional category. To tackle this difficulty, a multiresolution direction classification is proposed to achieve the more accurate direction estimation. This classification is a two-level windowing process. The first-level process is the original voting mechanism which provides a coarse estimation for the edge

direction and then determines the selected nested region between two adjacent direction categories. The second-level process is a fine estimation for the edge direction based on four finer directional categories belonging to the chosen nested region. The difference between any two adjacent finer directional categories is 5.625°. In simulation results, we will compare our multiresolution approach with Kwok's method [15] and show the improvement of our method.

Sometimes, a cell loss may cause a sequence of consecutive horizontal block losses when it contains a slice header, or a macroblock header or a sequence of block data. A sliding block iteration method is proposed to conceal the contiguous block loss by using the multiresolution multidirectional interpolation block-by-block. First, the damaged left-most block is recovered based on its seven neighboring correct blocks. Next, the recovered block is treated as the correct neighboring block adjacent to the second left-most damaged block and can be applied for multidirectional interpolation. In the same time, the similar recovery process is performed from the right-most damaged block to the left one. The sliding block iteration is terminated when all the damaged blocks have been recovered. The method is also valid for color MPEG videos by applying the iteration to each of Y-, U-, and V-blocks, independently. Another method to conceal consecutive block losses is to apply block-interleaving scheme to isolate the block loss. However, it may cause encoding and reconstruction delay [14], [24]. Sometimes, it will become invalid when the consecutive block losses are caused by the bit errors in either slice header or macroblock header.

B. Iterative Pattern Matching Algorithm for Temporal Error Concealment

The general approach for temporal error concealment is the temporal replacement [14], [17], [18]. In temporal replacement, damaged blocks in the current frame are replaced by the spatially corresponding ones in the previously decoded reference frame with motion compensation if motion information is available. Narula and Lim [18] have shown that the estimate of motion vector in the lost block (i.e., macroblock of size 16 × 16 in MPEG-2) can be obtained by taking the median of all eight adjacent correct motion vectors. It should be mentioned that the motion vector is defined in a macroblock sense. Therefore, the damaged macroblock can be replaced by a correct or previously concealed macroblock in the reference picture based on the estimate. However, this method does not work well when high-frequency information such as edges, contours, and fine textures appear in the macroblock. To tackle this difficulty, an iterative pattern matching algorithm is proposed to improve the performance of temporal replacement. First, the damaged macroblock is recovered based on the estimated median motion vector. This leads to a coarse recovered marcroblock. In the spatial domain, the coarse recovered macroblock with 16 × 16 pixels is further divided into 16 subblocks with each having 4 × 4 pixels. Since the corner subblocks tend to be more correlated with their three immediate neighboring correct subblocks, each corner subblock can be combined with its three neighboring correct subblocks to construct an estimated larger block of size 8 × 8. This estimated block is further replaced by a block in the reference picture which has the minimum mean square error deviation to match the estimated block in the current frame. One can find such a block by using block matching algorithm [14]. The corner subblocks belonging to the best-matching blocks are then treated as the correct subblocks and can be applied for the next pattern matching. Finally, those recovered subblocks are then combined to yield the fine recovered marcoblock. More details of the iterative pattern matching algorithm can be found in [33]. The pattern matching process is valid for the recovery of the damaged macroblocks belonging to a B-frame. For a B-frame, two recovered macroblocks may be obtained by using the pattern matching iteration with respect to the previous and the next reference pictures, respectively. Finally, the damaged macroblock of a B-frame has been concealed by taking the average of these two recovered macroblocks.

The iterative pattern matching can be extended to conceal the consecutive lost macroblocks [33]. The recovery process is performed in the right direction and left direction simultaneously until all the damaged macroblocks have been recovered.

VIII. Simulation Results

The channel model described in this paper is identical to Model-I employed in [25]. In this model, the variances of the Rayleigh path gains are the same for all MPEG users and equal to −14.2 dB (0.038). Additionally, the maximum number of resolved multipaths for all users is equal to 4, i.e., $L = 4$. The channel noise is set to be $(E_b/N_0) = 25$ dB. The multicode CDMA system has a transmission rate of $r_B = 64$ kb/s, a processing gain of $N_c = 128$, and a bandwidth of 10 MHz [10]. Its corresponding PN and orthogonal spreading sequences are chosen as the Gold sequence with a period equal to $(2^{31} - 1)$ and the WH code with a period of 128. For CDMA receiver, it has an MRC of order $L_d = 4$. For the interleaving scheme, the outercoded data are interleaved over 215 bits for I-frames (223 bits for P-frames or 231 bits for B-frames), and the inner-coded data plus the coded ATM header data are interleaved over 20 cells.

To evaluate the performance of multiple MPEG video transmission via multicode CDMA systems, a high bit-rate Flower Garden and a medium bit-rate Table Tennis are considered as a typical example in the simulation. From section V, it is found that there are five frame combinations, i.e., (I,B), (B,I), (P,B), (B,P), and (B,B) in the optimal frame interleaving pattern, where the first and second components belong to Table Tennis and Flower Garden, respectively. Thus, (B,I) is the maximum two-user bit-rate frame combination. The average WH code numbers for an I-frame in Flower Garden and for a B-frame in Table Tennis are found to be $(\overline{N}_I)_{FG} = 62$ and $(\overline{N}_B)_{TT} = 5$, respectively, according to the ATM cell generation

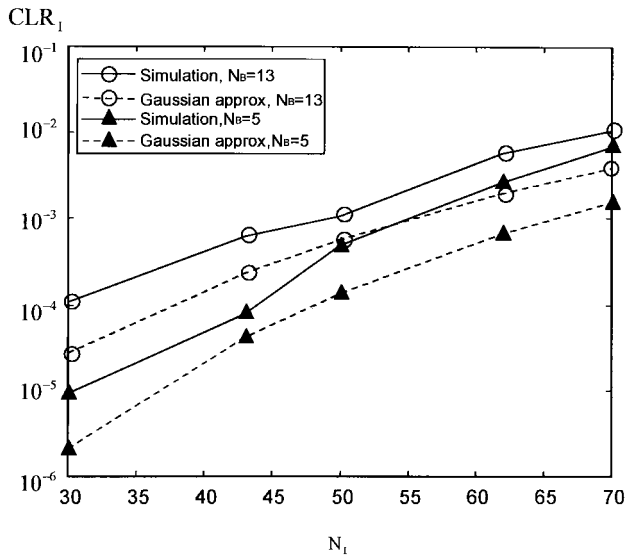

Fig. 8. CLR for an I-frame versus a varying WH code number N_I due to the interfering B-frame with either $N_B = 13$ or 5.

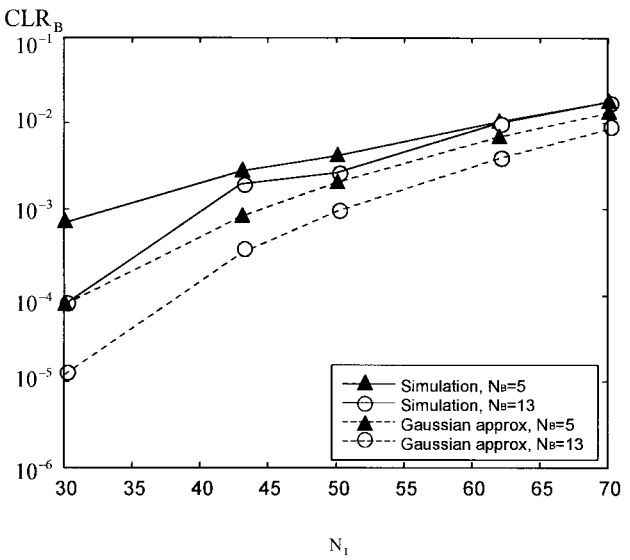

Fig. 9. CLR for a B-frame with either $N_B = 13$ or 5 due to the interfering I-frame with a varying WH code N_I.

method proposed in Section III with $(\overline{R}_{c,I})_{FG} = 0.7388$ and $(\overline{R}_{c,B})_{TT} = 0.6509$. For the second maximum two-user bit-rate frame combination, i.e., (I,B), the average WH code numbers for an I-frame in Table Tennis and for a B-frame in Flower Garden are $(\overline{N}_I)_{TT} = 43$ and $(\overline{N}_B)_{FG} = 13$, respectively when their corresponding code rates are $(\overline{R}_{c,I})_{TT} = 0.6957$ and $(\overline{R}_{c,B})_{FG} = 0.7548$. Fig. 8 shows a comparison between the simulation values and Gaussian approximation for average cell loss rate for an I-frame, CLR_I, with a varying WH code number, N_I, due to the interfering B-frame with either $N_B = 13$ or 5 when $K = 2$. Note that Fig. 8 highlights a generic representation for CLR_I, where the values of N_I and N_B represent, respectively, the I- and B-frames belonging to either Table Tennis or Flower Garden. CLR_I at a point $(N_I, N_B) = (43, 13)$ represents the average CLR with a value of 6.27×10^{-4} for an I-frame $(\overline{N}_I = 43)$ in Table Tennis due to the interfering B-frame $(\overline{N}_B = 13)$ in Flower Garden. On the other hand, CLR_I at $(N_I, N_B) = (62, 5)$ denotes the average CLR with a value of 2.688×10^{-3} for an I-frame $(\overline{N}_I = 62)$ in Flower Garden due to the interfering B-frame $(\overline{N}_B = 5)$ in Table Tennis. Thus, the average number of cell losses in an I-frame (cell loss number per I-frame) belonging to Table Tennis is equal to 0.611 $(= 6.27 \times 10^{-4} \times 975)$ since the average number of ATM cells generated from its I-frame (ATM cell number per I-frame) is found to be 975. The average cell loss number per I-frame for Flower Garden equals 3.79 $(2.688 \times 10^{-3} \times 1410)$ since its average ATM cell number per I-frame is 1410. On the contrary, Fig. 9 shows the average CLR for a B-frame with either $N_B = 13$ or $N_B = 5$ due to the interfering I-frame with a varying N_I. In contrast to Fig. 8, CLR_B at $(N_I, N_B) = (43, 13)$ represents the average CLR with a value of 2.0×10^{-3} for a B-frame $(\overline{N}_B = 13)$ in Flower Garden due to the interfering I-frame $(\overline{N}_I = 43)$ in Table Tennis. Therefore, the average cell loss number per B-frame for Flower Garden equals 0.6 since its average ATM cell number per B-frame is 300. Similarly, the average cell loss number per B-frame for Table Tennis equals 1.622 since CLR_B at $(N_I, N_B) = (62, 5)$ is 1.0385 $\times 10^{-2}$ and its average ATM cell number per B-frame is 120. Based on the above analysis, it is seen that the average number of ATM cell losses in either I- or B-frames belonging to either Flower Garden or Table Tennis is in the order of $O(1)$. As a result, the appropriate maximum allowable numbers of WH codes assigned to I- and B-frames could be chosen as $N_{I,\max} = 62$ and $N_{B,\max} = 13$, respectively, by considering the compromise between the above two cases.

Considering the third maximum two-user bit-rate frame combination, i.e., (B,P), and the fourth maximum two-user bit-rate frame combination, i.e., (P,B) according to the similar analysis, their maximum allowable WH code numbers can be chosen as $N_{P,\max} = 54$ and $N_{B,\max} = 13$ since the average WH code numbers for a P-frame and for a B-frame in the highest bit-rate Flower Garden are, respectively, $(\overline{N}_P)_{FG} = 54$ and $(\overline{N}_B)_{FG} = 13$. It is found that the average cell loss number per frame for a P-frame in Flower Garden and for a B-frame in Table Tennis are equal to 0.5855 $(= 4.76 \times 10^{-4} \times 1230)$ and 0.5804 $(= 4.867 \times 10^{-3} \times 120)$, respectively. According to above analysis, these maximum allowable WH code numbers for I- , P-, and B-frames may be directly chosen as the WH code numbers derived from their respective average bit-rates in the highest average bit-rate MPEG video stream. Meanwhile, actually, these maximum allowable WH numbers could be obtained in accordance with the highest peak bit rate for each frame in the highest average bit-rate MPEG video over the presentation time period. This would result in the larger value of maximum allowable WH number for each frame. More WH codes are able to provide more virtual channels for the transmission of multiple MPEG videos in order to carry all the picture data to receivers within a short time period. However, the larger maximum allowable WH

number also creates the larger CLR for each picture frame and then degrades the picture quality further. Moreover, a large portion of WH codes remains unused when multiple low bit-rate B-frames are transmitted over the multicode CDMA channels. For the case of maximum allowable WH numbers in the average bit-rate manner, it is suggested that an amount of low-priority data in a picture frame with higher peak bit-rate should be abandoned according to the spreading code assignment mechanism in order to achieve the reasonable CLR when its bit-rate is greater than the average bit-rate at a specific time instant. For example, the picture quality for a B-frame in Flower Garden is maintained at the performance of $\text{PSNR}_Y = 28.154, \text{PSNR}_U = 35.58$, and $\text{PSNR}_V = 33.341$ when 60% of AC coefficients have been abandoned. Thus, the value of $(\overline{N}_B)_{FG}$ is reduced from 13 to 7. Similarly, $(\overline{N}_B)_{TT}$ becomes three when 60% of AC coefficients have been abandoned. Its picture quality is still maintained at the performance of $\text{PSNR}_Y = 33.602, \text{PSNR}_U = 39.343$, and $\text{PSNR}_V = 41.254$. Thus, the value of $N_{B,\max}$ is reduced from 13 to 7. From the above discussion, it ensures that our spreading code assignment mechanism is able to achieve each picture frame with a reasonable average ATM cell loss number per frame proportional to $O(1)$ when the maximum allowable WH code numbers in the average bit-rate manner are treated as the input to the assignment mechanism. As a result, both the cell loss number per frame and received picture quality performance for each picture frame with higher peak bit-rate are still achieved at acceptable levels when the low-priority data in each macroblock of these frames have been abandoned according to our assignment mechanism.

The second major factor in picture degradation is caused by the transmission error in the payload containing MPEG video data; even the delivery of its associated ATM cell is successful. The impact of transmission error in MPEG videos seems very significant in the picture quality since both the DCT coefficients and macroblock headers are encoded using run-length and VLC. In this paper, we make a modification for the original MPEG codec developed by ISO/IEC [27] to localize the error in a picture frame. For example, a DCT coefficient is lost if a single bit error occurs in that coefficient. A loss of the complete macroblock occurs when a single bit error appears in its header. Moreover, a slice of subsequent macroblock may be destroyed when a bit error occurs in a slice header. For P- and B-frames, a bit error in a motion vector may result in the corruption of this macroblock and the following predicted macroblocks since motion vectors are differentially encoded for the intercoded macroblocks in the same slice. The adaptive FEC code combining has been proposed to protect the payload in accordance with the importance of data types in MPEG videos. An extra more powerful outer FEC code is applied to the more valuable information, i.e., slice header, macroblock header, and DC coefficients in I-frames, or slice header, macroblock header, motion vectors, and DC coefficients in either P- or B-frames, thereby spending more channel coding bits on it. The higher frequency DCT coefficients are visually less important than the DC coefficients and have very little impact on video quality.

Fig. 10. Received I-frame (frame 54) in Flower Garden due to the interfering B-frame (frame 55) in Table Tennis.

Our system has been evaluated over 150 frames of both Flower Garden and Table Tennis. We particularly choose the worst case of a cell loss containing the slice header and a bit error in the macroblock header when the ATM cell is successful. The worse case of the maximum two-user bit-rate frame combination, (B,I), occurs in the fifty-fouth frame (I-frame) in Flower Garden and the fifty-fifth frame (B-frame) in Table Tennis. Fig. 10 shows the received I-frame (frame 54) in Flower Garden with six lost areas. Observing Fig. 10 from top to bottom, it is found that the second, fourth, and sixth lost areas (black areas) are caused by the three cell losses, and the first, third, and fifth lost areas are caused by the bit errors in the payload when its ATM cell is successful. Especially, the cell loss containing a slice header results in the loss of a slice of subsequent macroblocks in the second area. The third lost area is caused by a bit error in macroblock header. The damage rates for DC and AC coefficients are found to be 0.1515 and 13.15%, respectively. The first and fifth areas are lost when both the DC and AC coefficients have been damaged simultaneously. Moreover, from Fig. 10, it is seen that the remaining area in the picture seems visually good even 13.15% of AC coefficients have been damaged. As a result, this verifies the effectiveness of the adaptive FEC code combining for high priority data (macroblock header and DC coefficients). Fig. 11 illustrates the received B-frame (frame 55) in Table Tennis with three lost areas, where the first lost area is caused by a cell loss containing a slice header and the other two lost areas are caused by the bit errors in the payload (macroblock header and motion vectors). DC coefficients did not have any damage. The damage rate for AC coefficients is 6.867%. Fig. 12 shows the recovered I-frame (frame 54) in Flower Garden by the multiresolution multidirectional interpolation techniques. The picture quality of Fig. 12 is improved at the performance of $\text{PSNR}_Y = 21.729\,456$, $\text{PSNR}_U = 32.537\,960$, and $\text{PSNR}_V = 29.144\,493$. On the other hand, Fig. 13 illustrates the recovered B-frame (frame 55) in Table Tennis

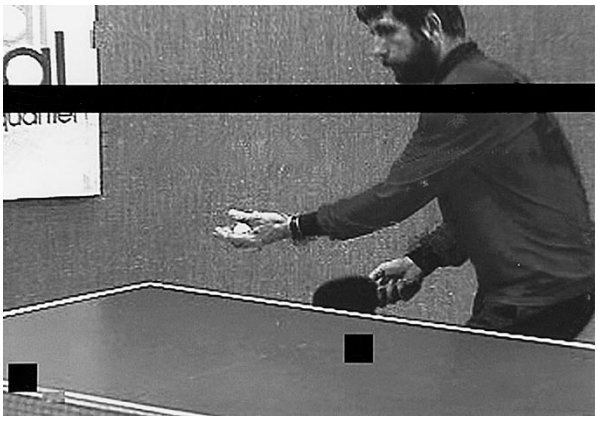

Fig. 11. Received B-frame (frame 55) in Table Tennis due to the interfering I-frame (frame 54) in Flower Garden.

Fig. 12. Recovered I-frame (frame 54) in Flower Garden by multiresolution multidirectional interpolation.

by the iterative pattern matching method. The picture quality performance of Fig. 13 is $\text{PSNR}_Y = 31.444\,981$, $\text{PSNR}_U = 33.673\,79$, and $\text{PSNR}_V = 37.155\,289$. It is found that the received I-frame (frame 54) in Table Tennis and the received B-frame (frame 53) in Flower Garden belong to the second maximum two-user bit-rate frame combination, (I,B) [29]. There are four lost areas for each of received I- and B-frames, where two of them are caused by the loss in their cells. For the I-frame in Table Tennis, two macroblock headers (second and fourth lost areas) have been damaged when their associated ATM cells are successful. The damage rates for its DC and AC coefficients are equal to 0.0758 and 2.575%, respectively. However, they have not been damaged simultaneously. On the other hand, there are a damaged macroblock header (first lost area), a damaged motion vector (third lost area), and no damage in DC coefficients for the B-frame in the Flower Garden. The damage rate for its AC coefficients is 8.490%. Reference [29] has shown that the PSNR's of both the recovered frames are $\text{PSNR}_Y = 32.620\,167$, $\text{PSNR}_U = 35.651\,696$, and $\text{PSNR}_V = 39.462\,460$ for the recovered I-frame, and $\text{PSNR}_Y = 21.847\,149$, $\text{PSNR}_U = 31.926\,815$, and $\text{PSNR}_V = 27.735\,929$ for the recovered B-frame. For the worst case of the third maximum two-user bit-rate frame combination, (B,P), it has been found that the received

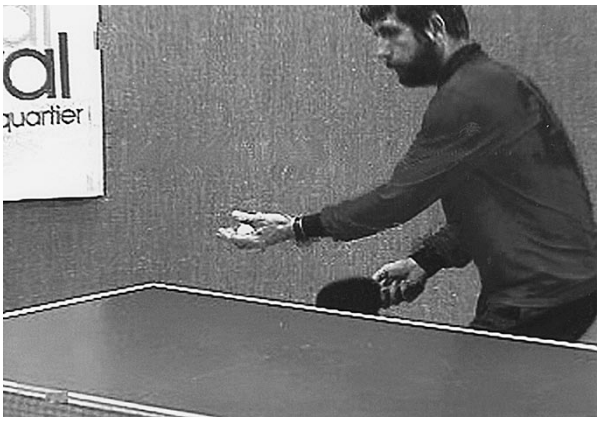

Fig. 13. Recovered B-frame (frame 55) in Table Tennis by iterative matching method.

P-frame (frame 57) in Flower Garden and the received B-frame (frame 58) in Table Tennis have the identical number of lost areas, where three lost areas appear in each figure. There are two cell losses (second and third lost areas), a damaged motion vector (first lost area) and no damage in both the macroblock headers and DC coefficients belonging to the P-frame in Flower Garden. The damage rate for its AC coefficients is 2.56%. In contrast to Flower Garden, there are a single cell loss (second lost area), two damaged macroblock headers (first and third lost areas) and no damage in the motion vectors for the B-frame in Table Tennis. The damage rates for its DC and AC coefficients are 0.0515 and 5.1%, respectively. Only the iterative pattern matching method is applied to either received P- or B-frame. The recovered P- and B-frames are improved at the performance of $\text{PSNR}_Y = 21.077\,045$, $\text{PSNR}_U = 30.912\,437$, and $\text{PSNR}_V = 27.098\,217$, and $\text{PSNR}_Y = 31.538\,477$, $\text{PSNR}_U = 33.142\,929$, and $\text{PSNR}_V = 36.408\,348$, respectively [29]. Here, we ignore both the fourth maximum two-user bit-rate and minimum two-user bit-rate frame combinations, i.e., (P,B) and (B,B) which seem less important in the evaluation of our system. Finally, it should be mentioned that the reference pictures used to recover either P- or B-frame by using the iterative pattern matching method are either the previously recovered I- or P-frame or both.

IX. Conclusion and Future Research Work

A MPEG-2 video transmission over ATM-based multicode CDMA channels is investigated in this paper. Two separate FEC code schemes are applied to the header and payload of a ATM cell, respectively. A shortened BCH(31,16) code is proposed to effectively protect the ATM cell header in order to ensure the average number of ATM cell losses in a frame be in the the order of $O(1)$. Moreover, an adaptive FEC code combining is used to provide the good protection for the payload data. Especially, an additional outer FEC code is proposed to increase the error protection capability for the high priority data in the payload with the maximization of its code rate. The spreading code assignment mechanism provides the

sufficient number of virtual channels for the delivery of multiple MPEG videos within a desired frame time period and at an acceptable cell loss number per frame. Finally, the information loss due to cell loss can be concealed by using both the multiresolution multidirectional interpolation and iterative pattern matching methods. The effectiveness of overall system architecture has been verified by two typical MPEG test sequences. It should be noted that the design concept of our system is not restricted to the MPEG-2 videos and also suitable for the other benchmark H.261 and H.263 video codecs as well as the next in the line of MPEG standards, MPEG-4 when the outer FEC code combing, spreading code assignment mechanism, and error concealment techniques have been modified according to their characteristics. In our companion paper [34], we found that our system with a little modification is particularly suitable for Sarnoff's MPEG-4 codec [35] which is actually a combination of wavelet-based multiresolution coding and motion-compensated coding. The multiresolution coding creates the priority for subimages in the spatial domain, whereas the motion-compensated coding provides the priority for picture frames in the temporal domain. Thus, an adaptive FEC scheme with UEP is applied to the payload in accordance with three priority categories, i.e., priority for each picture frame in both the spatial/temporal domain and the importance of data types belonging to the frame. This would lead to the almost best performance in both bandwidth utilization and received picture quality via wireless CDMA channels. Currently, we are trying to refresh our system. This new version has a number of improvements: 1) applying the turbo FEC code to the design of wireless ATM cell; 2) more powerful error resilient video coding that has been designed to be resilient against the multipath fading, interference, and AWGN; 3) reconfigurable architecture for the wideband CDMA (WCDMA) in UMTS/IMT-2000; 4) more cost-effective spreading code management incorporated with the rate and quantization size control in each video codec; 5) more powerful multiple-video traffic regulation and scheduling techniques; and 6) more powerful error concealment methods.

REFERENCES

[1] K. Miya, M. Waranabe, M. Hayashi, T. Kitade, O. Kato, and K. Homma, "CDMA/TDD cellular systems for the 3rd generation mobile communication," in *Proc. IEEE VTC'97*, Phoenix, AZ, pp. 820–824.

[2] S. Onoe, K. Ohno, K. Yamagata, and T. Nakamura, "Wideband-CDMA radio control techniques for third-generation mobile communication systems," in *Proc. IEEE VTC'97*, Phoenix, AZ, pp. 835–844.

[3] D. Raychaudhuri and N. Wilson, "ATM based transport architecture for multiservices wireless personal communication network," *IEEE J. Select. Areas Commun.*, vol. 12, pp. 1401–1414, Oct. 1994.

[4] D. LeGall, "MPEG: A video compression standard for multimedia applications," *Commun. ACM*, vol. 34, no. 4, pp. 46–58, 1991.

[5] D. Moore and M. Rice, "Variable rate error control for wireless ATM network," in *Proc. ICC'95*, 1995, pp. 988–992.

[6] M. J. Mctiffin, A. P. Hulbert, T. J. Ketseoglou, W. Heimsch, and G. Crisp, "Mobile access to an ATM network using a CDMA air interface," *IEEE J. Select Areas Commun.*, vol. 12, pp. 900–908, June 1994.

[7] J. B. Cain and D. N. McGregor, "A recommended error control architecture for ATM networks with wireless links," *IEEE Select. Areas Commun.*, vol. 15, pp. 16–28, Jan. 1997.

[8] J. Zhang, M. R. Frater, J. F. Arnold, and T. M. Percival, "MPEG2 video services for wireless ATM networks," *IEEE Select. Areas Commun.*, vol. 15, pp. 119–128, Jan. 1997.

[9] C.-L. I, G. P. Pollini, L. Ozarow, and R. D. Gitlin, "Performance of multi-code CDMA wireless personal communication networks," in *Proc. 1995 IEEE 45th Vehicular Technology Conference*, Chicago, IL, pp. 907–911.

[10] M. H. Fong, V. K. Bhargava, and Q. Wang, "Concatenated orthogonal/PN spreading sequences and their application to cellular DS-CDMA Systems with integrated traffic," *IEEE J. Select. Areas Commun.*, vol. 14, pp. 547–557, Apr. 1996.

[11] P. R. Chang, "Spreading spectrum CDMA system for subband image transmission," *IEEE Trans. Veh. Technol.*, vol. 46, pp. 80–95, Feb. 1997.

[12] Y. Q. Zhang and X. Lee, "Performance of MPEG Codes in the presence of errors," *J. Visual Commun. Image Representation*, vol. 5, no. 4, pp. 379–387, Dec. 1994.

[13] Y. Wang, Q. F. Zhu, and L. Shaw, "Maximally smooth image recovery in transform coding," *IEEE Trans. Commun.*, vol. 41, pp. 1544–1551, Oct. 1993.

[14] I. W. Tsai and C. L. Huang, "Hybrid cell loss concealmet methods for MPEG-II- based packet video," *Signal Processing: Image Commun.*, vol. 9, no. 2, pp. 99–124, Jan. 1997.

[15] W. Kwok and H. Sun, "Multi-directional interpolation for spatial error concealment," *IEEE Trans. Consumer Electron.*, vol. 39, pp. 455–460, Aug. 1993.

[16] X. Lee, Y. Q. Zhang, and A. Leon-Garcia, "Information loss recovery for block-based image coding techniques—A fuzzy logic approach," *IEEE Trans. Image Processing*, vol. 4, pp. 259–273, Mar. 1995.

[17] S. Aign and K. Fazel, "Error detection & concealment measures in MPEG-2 video decoder," in *Proc. Int. Workshop HDTV'94*, Torino, Italy, pp. 612–619.

[18] A. Narula and J. S. Lim, "Error concealment techniques for an all-digital high-definition television system," in *Proc. SPIE*, vol. 2094, 1993, pp. 415–501.

[19] S. M. Lei, "Forward error correction codes for MPEG2 over ATM," *IEEE Trans. Circuits Syst. Video Technol.*, vol. 4, pp. 200–203, Apr. 1994.

[20] G. C. Clark, Jr. and T. B. Cain, *Error-Correction Coding for Digital Communications*. New York: Plenum, 1981.

[21] V. Parthasarathy, J. W. Modestino, and K. S. Vastola, "Design of transport coding scheme for high-quality video over ATM networks," *IEEE Trans. Circuits Syst. Video Technol.*, vol. 7, pp. 358–376, Apr. 1997.

[22] J. G. Prokis, *Digital Communications*. New York: McGraw-Hill, 1983.

[23] H. Ohta and T. Kitami, "A cell loss recovery method using FEC in ATM networks," *IEEE Select. Areas Commun.*, vol. 9, pp. 1471–1483, Dec. 1991.

[24] H. Liu and M. El Zarki, "Transmission of video telephony images over wireless channels," *Wireless Networks*, vol. 2, no. 2, pp. 219–228, July 1996.

[25] M. Kavehrad and B. Ramamurthi, "Direct-sequence spread spectrum with DPSK modulation and diversity for indoor wireless communications," *IEEE Trans. Commun.*, vol. COM-35, pp. 224–236, Feb. 1987.

[26] M. K. Ozkan, M. I. Sezan, and A. M. Tekalp, "Adaptive motion-compensation filtering of noisy image sequences," *IEEE Trans. Circuits Syst. Video Technol.*, vol. 3, pp. 277–290, Aug. 1993.

[27] *Generic Coding of Moving Pictures and Associated Audio Information: Video*, ISO/IEC Int. Standard 13818-2, 1995.

[28] M. B. Pursley, "Spreading spectrum mutiple access communications," in *Multi-User Communication Systems*. New York: Springer-Verlag, 1981, pp. 139–189.

[29] P. R. Chang, "Wireless ATM-based multi-code CDMA transport architecture for MPEG2 video transmission," in *Proc. 10th Int. Conf. Wireless Communications*, Calgary, Alta., Canada, July 1998, pp. 547–561.

[30] E. K. Hall and S. G. Wilson, "Design and analysis of turbo codes on Rayleigh fading channels," *IEEE J. Select. Areas Commum.*, vol. 16, pp. 160–174, Feb. 1998.

[31] J. D. Andersen, "Turbo coded extended with outer BCH code," *Electron. Lett.*, vol. 32, no. 22, pp. 2059–2060, Oct. 1996.

[32] M. Krunz and S. K. Tripathi, "Impact of video scheduling on

bandwidth allocation for multiplexed MPEG streams," *Multimedia Syst.*, vol. 5, no. 6, pp. 347–357, Dec. 1997.
[33] P. R. Chang, "Error concealment techniques for 3D videos via wireless CDMA networks," submitted for publication.
[34] P. R. Chang and C. F. Lin, "Design of multi-code CDMA systems for 3D stereoscopic video over wireless ATM networks," *IEEE Trans. Veh. Technol.*, to be published.
[35] Y. Q. Zhang, S. A. Martucci, I. Sodagar, and T. Chiang, "A zerotree wavelet video coder," special issue on MPEG-4, *IEEE Trans. Circuits Syst. Video Technol.*, vol. 7, pp. 109–118, Feb. 1997.

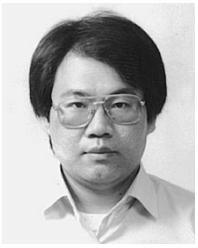

Po-Rong Chang (Member, IEEE) received the B.S. degree in electrical engineering from National Tsing-Hua University, Hsin-Chu, Taiwan, in 1980, the M.S. degree in communication engineering from National Chiao-Tung University, Hsin-Chu, Taiwan, in 1982, and the Ph.D. degree in electrical engineering from Purdue University, West Lafayette, IN, in 1988.

From 1982 to 1984, he was a Lecturer in the Chinese Air Force Telecommunication and Electronics School. From 1984 to 1985, he was an Instructor of Electrical Engineering at National Taiwan Institute of Technology, Taipei. From 1989 to 1990, he was a Project Leader in charge of the SPARC Chip Design Team at ERSO of Industrial Technology and Research Institute, Chu-Tung, Taiwan. Currently, he is a Professor of Communication Engineering at National Chiao-Tung University, Hsin-Chu, Taiwan. His current interests include wide-band CDMA systems, wireless multimedia communications, fuzzy neural networks, and low-power design for wireless communications.

Dr. Chang was the recipient of the Best Paper Award in quality control for semiconductor manufacturing, Taiwan, in 1990.

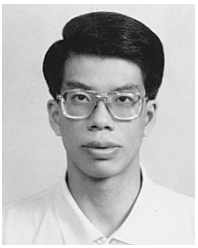

Chin-Feng Lin was born in Taiwan in 1965. He received the B.S. degree in electrical engineering from Chung-Yung University, Taipei, Taiwan, in 1996 and the M.S. degree in electrical engineering from Chung-Hua University, Hsin-Chu, Taiwan. He is currently pursuing the Ph.D. degree in communication engineering at National Chiao-Tung University, Hsin-Chu, Taiwan.

His research interests include CDMA systems and wireless multimedia communications.